

Isolevuglandin-modified phosphatidylethanolamine is metabolized by NAPE-hydrolyzing phospholipase D

Lilu Guo,* Stephen D. Gragg,* Zhongyi Chen,* Yongqin Zhang,* Venkataraman Amarnath,[†] and Sean S. Davies^{1,*,*§}

Division of Clinical Pharmacology,* and Departments of Pathology[†] and Pharmacology,[§] Vanderbilt University, Nashville, TN

Abstract Lipid aldehydes including isolevuglandins (IsoLGs) and 4-hydroxynonenal modify phosphatidylethanolamine (PE) to form proinflammatory and cytotoxic adducts. Therefore, cells may have evolved mechanisms to degrade and prevent accumulation of these potentially harmful compounds. To test if cells could degrade isolevuglandin-modified phosphatidylethanolamine (IsoLG-PE), we generated IsoLG-PE in human embryonic kidney 293 (HEK293) cells and human umbilical cord endothelial cells and measured its stability over time. We found that IsoLG-PE levels decreased more than 75% after 6 h, suggesting that IsoLG-PE was indeed degraded. Because *N*-acyl phosphatidylethanolamine-hydrolyzing phospholipase D (NAPE-PLD) has been described as a key enzyme in the hydrolysis of *N*-acyl phosphatidylethanolamine (NAPE) and both NAPE and IsoLG-PE have large aliphatic headgroups, we considered the possibility that this enzyme might also hydrolyze IsoLG-PE. We found that knockdown of NAPE-PLD expression using small interfering RNA (siRNA) significantly increased the persistence of IsoLG-PE in HEK293 cells. IsoLG-PE competed with NAPE for hydrolysis by recombinant mouse NAPE-PLD, with the catalytic efficiency (V_{max}/K_m) for hydrolysis of IsoLG-PE being 30% of that for hydrolysis of NAPE. LC-MS/MS analysis confirmed that recombinant NAPE-PLD hydrolyzed IsoLG-PE to IsoLG-ethanolamine. **■** These results demonstrate that NAPE-PLD contributes to the degradation of IsoLG-PE and suggest that a major physiological role of NAPE-PLD may be to degrade aldehyde-modified PE, thereby preventing the accumulation of these harmful compounds.—Guo, L., S. D. Gragg, Z. Chen, Y. Zhang, V. Amarnath, and S. S. Davies. **Isolevuglandin-modified phosphatidylethanolamine is metabolized by NAPE-hydrolyzing phospholipase D.** *J. Lipid Res.* 2013. 54: 3151–3157.

Supplementary key words isoketal • *N*-acyl phosphatidylethanolamine • cytotoxicity • inflammation • oxidative stress • *N*-acyl ethanolamine

This work was supported by funds from the Vanderbilt Department of Pharmacology (S.S.D.) and National Institutes of Health Grants OD-003137-01 (S.S.D.), P30 ES-000267 (Vanderbilt Center in Molecular Toxicology), and ULI RR-024975 (Vanderbilt Institute for Clinical and Translation Research).

Manuscript received 19 July 2013 and in revised form 6 September 2013.

Published, JLR Papers in Press, September 9, 2013

DOI 10.1194/jlr.M042556

Oxidative stress has been implicated in atherosclerosis, diabetes, neurodegenerative diseases, and various cancers. Peroxidation of lipids generates a number of highly reactive aldehydes including isolevuglandins (IsoLGs) (1, 2). IsoLGs induce a variety of cellular responses related to the pathophysiology of human diseases, including increased macrophage uptake of LDL, activation of platelet aggregation, inhibition of sodium and potassium channels, inhibition of proteasome function, induction of proinflammatory genes, and cytotoxicity (3–6).

Recent studies show that the proinflammatory and cytotoxic effects of lipid aldehydes such as IsoLGs are mediated in part by their modification of the headgroups of phosphatidylethanolamines (PEs) (7–9). Isolevuglandin-modified phosphatidylethanolamine (IsoLG-PE) levels increase during a number of pathological conditions (10–12), suggesting that cellular systems that normally degrade IsoLG-PE may become dysfunctional during these conditions. We therefore sought to characterize the processes by which cells normally degrade IsoLG-PE.

N-acyl phosphatidylethanolamine hydrolyzing phospholipase D (NAPE-PLD) catalyzes the hydrolysis of *N*-acyl phosphatidylethanolamines (NAPEs) to *N*-acyl ethanolamines (NAEs) such as anandamide (13). Although both NAPE-PLD and canonical phospholipase Ds (PLDs) (PLD1 and PLD2) hydrolyze the headgroups at the phosphodiester bond of phospholipids, these two classes of PLDs do not share structural or enzymatic homology. Unlike the canonical PLDs, NAPE-PLD does not transphosphatidylate phospholipids, nor does it hydrolyze phosphatidylcholine (PC) or unmodified PE (14–16). Instead, NAPE-PLD hydrolyzes NAPE with *N*-acyl chains of 4 to 20 carbons, with

Abbreviations: al-PE, aldehyde-modified phosphatidylethanolamine; DPPE, 1-palmitoyl-2-palmitoyl-sn-glycero-3-phosphoethanolamine; Etn, ethanolamine; HEK293, human embryonic kidney 293; HUVEC, human umbilical cord endothelial cell; IsoLG, isolevuglandin; IsoLG-PE, isolevuglandin-modified phosphatidylethanolamine; MRM, multiple reaction monitoring; NAE, *N*-acyl ethanolamine; NAPE, *N*-acyl phosphatidylethanolamine; NAPE-PLD, *N*-acyl phosphatidylethanolamine hydrolyzing phospholipase D; NBD, (7-nitro-2-*l*,3-benzoxadiazol-4-yl) amino; PA, phosphatidic acid; PC, phosphatidylcholine; PE, phosphatidylethanolamine; PLD, phospholipase D; small interfering RNA, siRNA.

¹To whom correspondence should be addressed.

e-mail: sean.davies@vanderbilt.edu

C12:0NAPE having the highest hydrolysis rate (15). While NAPE-PLD^{-/-} mice have significantly increased levels of NAPE and reduced levels of NAEs such as oleoylethanolamide and palmitoylethanolamide compared with wild-type mice, anandamide levels are not changed in NAPE-PLD^{-/-} mice (17), raising the possibility that the main physiological role of NAPE-PLD may be something other than endocannabinoid synthesis. Because both NAPE and IsoLG-PE have large aliphatic headgroups, we considered the possibility that NAPE-PLD is a critical catabolic enzyme for the catabolism of IsoLG-PE and other aldehyde-modified PEs (al-PEs). Our studies demonstrate that NAPE-PLD does indeed hydrolyze IsoLG-PE.

MATERIALS AND METHODS

Materials

All chemicals were purchased from Sigma-Aldrich unless otherwise noted. 1-Palmitoyl-2-palmitoyl-*sn*-glycero-3-phosphoethanolamine (DPPE) and 1-palmitoyl-2-(12-[(7-nitro-2-*l*,3-benzoxadiazol-4-yl)amino]dodecanoyl)-*sn*-glycero-3-phosphoethanolamine (NBD-PE) were purchased from Avanti Polar Lipids (Alabaster, AL). [²H₄] ethanolamine was purchased from Cambridge Isotopes (Cambridge, MA), isopropyl-β-D-thio-galactopyranoside and ampicillin from Research Products Institute (Mount Prospect, IL), and Calbiochem Protease Inhibitor cocktail set III from EMD Millipore (Billerica, MA). Ni-NTA agarose beads, FlexiTube GeneSolution GS222236 small interfering RNA (siRNA) for NAPE-PLD, and Transfect RNAi human/mouse starter kit were obtained from Qiagen (Valencia, CA). NAPE-PLD polyclonal antibody was purchased from Cayman Chemical (Ann Arbor, MI). Human embryonic kidney 293 (HEK293) cells were purchased from American Type Culture Collection (Manassas, VA). Endothelial cells derived from donated human umbilical cords (HUVECs) were a kind gift from Dr. Matthew Duvernay. Endothelial cell basal medium was purchased from Lonza Walkersville Inc. (Walkersville, MD). All solvents were HPLC grade and were purchased from EMD Millipore. IsoLG-PE, NBD-IsoLG-PE, IsoLG-ethanolamine (Etn), and [²H₄] IsoLG-Etn were synthesized as previously reported (8, 9). NBD-NAPE was synthesized similarly using NBD-PE rather than DPPE.

Cell experiments

HEK293 cells or HUVECs were cultured and grown on 100 mm dishes to >90% confluence as previously described (8, 9). For studies examining stability of IsoLG-PE, cells were washed twice with HBSS, incubated with 1 μM IsoLG in 10 ml HBSS for 1 h at 37°C to form IsoLG-PE, and then excess IsoLG removed by washing two times with DMEM. Cells were further incubated at 37°C for different times (0, 1, 6, or 24 h). At the appropriate time point, dishes were washed twice with HBSS, cells were scraped into 2 ml HBSS, internal standard added (C17NAPE, 0.1 nmol), and IsoLG-PE extracted with 2:1 chloroform/methanol for MS analysis.

For transfection of HEK293 cells with siRNA, Hs-NAPE-PLD-6, -7, and -8 siRNA and negative control siRNA (#1027280) from Qiagen were used. The degree of reduction of NAPE-PLD mRNA at 48 h after transfection was verified by real-time PCR and immunoblotting. After reverse transcription, cDNA was amplified using NAPE-PLD primers (NM_198990.4) and gene expression was normalized to the housekeeping gene, actin (ACTB, from Qiagen). For immunoblotting, endogenous proteins in lysates were detected using NAPE-PLD antibodies and normalized to actin (Santa Cruz, sc-1616-R).

IsoLG-Etn degradation studies in HEK293 cell lysate

Synthetic IsoLG-Etn was added to the cell lysate (200 μl). An aliquot of lysate (50 μl) was removed at incubation time 0, 1, and 6 h, followed by 2:1 chloroform/methanol extraction with [²H₄] IsoLG-Etn (0.1 nmol) as internal standard. The extracted lipids were dried under nitrogen and redissolved in 50 μl methanol for MS analysis.

MS analysis

IsoLG-PE was measured by LC-MS/MS after conversion to its phosphoglycero-ethanolamine derivative by base hydrolysis as previously described (9, 18). The initial adduct formed by IsoLG was a pyrrole adduct, which was subsequently converted to lactam and hydroxylactam in the presence of oxygen. Therefore, multiple reaction monitoring (MRM) for each adduct was performed (*m/z* 530.3 → 79.1, pyrrole; *m/z* 546.3 → 79.1, lactam; *m/z* 562.3 → 79.1, hydroxylactam; *m/z* 466.3 → 79.1, C17NAPE internal standard, 50 eV collision energy for each MRM) and the total IsoLG-PE was calculated by summing all three adducts. MS analysis of IsoLG-Etn and [²H₄]IsoLG-Etn was performed as previously described (8).

Expression and purification of recombinant NAPE-PLD

A nonexpression plasmid (pYX-Asc) containing the full-length cDNA for the mouse NAPE-PLD was purchased from Thermo Scientific Open Biosystems (CloneId: 5702354, catalog #MMM1013-9497346). Mouse NAPE-PLD was PCR-amplified using this plasmid as template and the following set of primers: sense primer, CGC GGA TGC ATG GAT GAG TAT GAG GAG AGC CAG; and antisense primer, GAG AGA TAT CTG ATG TTT CTT CAA AAG CTC TAT CAT CCG. The amplified DNA fragment was gel-purified and subcloned into pQE-80 His vector to generate plasmid pQE-80-PLDHis encoding C terminus 6× His tagged NAPE-PLD. pQE-80-PLDHis was transformed into *Escherichia coli* and after overnight induction with 1 mM isopropyl-β-D-thio-galactopyranoside at 30°C, the bacteria was pelleted and then lysed (lysis buffer: 50 mM NaH₂PO₄, 300 mM NaCl, 10 mM imidazole, 2 ul Calbiochem protease inhibitor cocktail set 3, and 1 mg/ml egg white lysozyme, pH 8). After centrifugation (20 min at 10,000 *g*), the supernatant was incubated with 2 ml Ni-NTA agarose beads along with 10 μl of Triton X-100 at 4°C for 1 h. Beads were washed twice (wash buffer: 50 mM NaH₂PO₄, 300 mM NaCl, and 10 mM imidazole, pH 8) and eluted with four 1 ml aliquots of elution buffer (50 mM NaH₂PO₄, 300 mM NaCl, and 250 mM imidazole). A portion of the lysate, wash, and elutions were run on SDS-PAGE and the gel visualized by staining with Coomassie blue. The third and fourth elution were combined and dialyzed to remove imidazole and concentrated using Millipore 30 kDa size exclusion filters so that the final purified enzyme was in HBSS buffer.

NAPE-PLD activity assays

To assess whether IsoLG-PE competitively inhibited NAPE hydrolysis by recombinant NAPE-PLD, reaction solutions were prepared in HBSS and contained the following components: 0–100 μM IsoLG-PE, 10 μM of NBD-NAPE, 5% ethanol, 1% *N*-octylglucoside, and 0.5 μg recombinant NAPE-PLD and incubated at 37°C for 2 h. Each reaction solution was then quenched by extraction with 2:1 chloroform/methanol solution. The organic layer was dried and redissolved in ethanol. The assay was analyzed by detecting the levels of NBD-phosphatidic acid (PA) using fluorescence-coupled HPLC (460 nm excitation, 534 nm emission). Samples were injected onto a C18 column (Grace Alltech; 4.6 mm × 150 mm, 5 μ) and products separated using a 34 min gradient from 40% solvent 1 (1 mM ammonium acetate in water) to 94% solvent 2 (1 mM ammonium acetate in reagent alcohol) with a

flow rate of 1 ml/min. Under these conditions, NBD-PA eluted at approximately 15 min and NBD-NAPE at approximately 27 min.

To determine the K_m and V_{max} values for NAPE-PLD, we measured the hydrolysis rate with 0–500 μM of NBD-IsoLG-PE or NBD-NAPE. A reaction solution containing 5% DMSO, 1% *N*-octylglucoside, and 1.5 ng/ μl NAPE-PLD was incubated with substrate at 37°C for 20 min, and then quenched by extraction with 2:1 chloroform/methanol solution. The level of NBD-PA formed was measured by fluorescence-coupled HPLC as above.

RESULTS

Cells degrade IsoLG-PE

To examine the stability of IsoLG-PE in cells, we treated HEK293 cells with IsoLG to generate IsoLG-PE, removed any unreacted IsoLG by washing, and then measured the persistence of IsoLG-PE over 6 h. We found that cellular IsoLG-PE levels decreased rapidly with time, so that less than 30% of the initial IsoLG-PE was present after 6 h (Fig. 1). While we chose HEK293 cells for our initial studies because of their rapid growth characteristic and ease of transfection, a more physiologically important site of IsoLG-PE action may be endothelial cells (9). We therefore also assessed the stability of IsoLG-PE in endothelial cells and found that IsoLG-PE levels also rapidly dropped

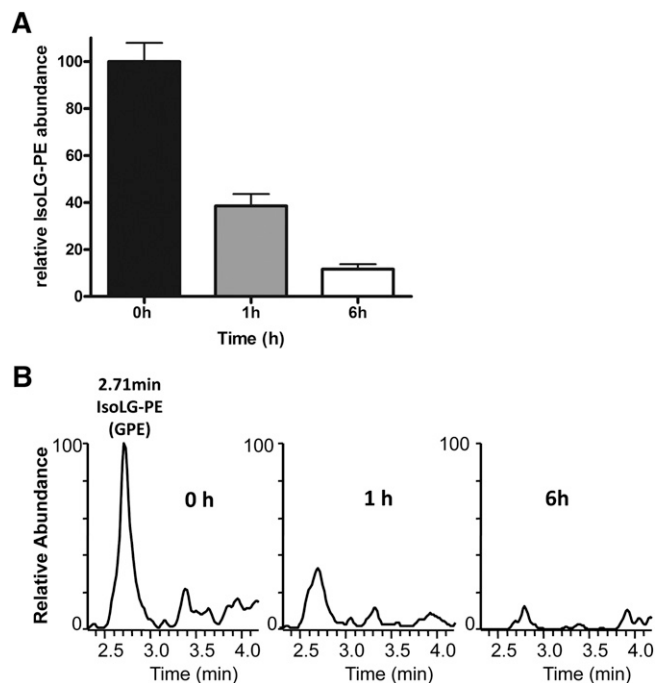


Fig. 1. HEK293 cells degrade IsoLG-PE. Confluent HEK293 cells were incubated with IsoLG (1 μM) for 1 h to form IsoLG-PE, excess IsoLG was removed by washing with DMEM, and IsoLG-PE levels were measured at 0, 1, or 6 h postwash by LC-MS after conversion to glycerophosphoethanolamine (GPE) derivative. A: Levels of IsoLG-PE in HEK293 cells decrease with time. Bars represent mean \pm SEM, $n = 3$, one-way ANOVA, $P < 0.0001$. B: Representative MRM-MS trace of IsoLG-PE (as GPE derivative) at each time point.

in these cells with less than 5% of IsoLG-PE present in HUVECs after 24 h (Fig. 2).

The loss of IsoLG-PE could be due either to hydrolysis by phospholipases or oxidative metabolism. Of note, our analytical technique (which uses base hydrolysis to eliminate the wide variety diversity of *sn*-1/*sn*-2 acyl chain combinations present in PE prior to mass spectrometric analysis) would not detect simple phospholipase A_2 hydrolysis of IsoLG-PE. Therefore, the dramatic decrease in IsoLG-PE must represent either degradation to phosphoethanolamide (by a phospholipase C activity) or ethanolamide products (by a PLD activity) or alternatively, β or omega oxidation of the IsoLG moiety.

Silencing NAPE-PLD inhibits metabolism of IsoLG-PE

We previously found that bacterial PLD rapidly hydrolyzed IsoLG-PE (8). We therefore considered the possibility that a mammalian PLD activity might also be responsible for IsoLG-PE hydrolysis. There are three known mammalian PLDs: PLD1, PLD2, and NAPE-PLD. The first two are PC-specific while NAPE-PLD catalyzes the hydrolysis of NAPE to NAE. Because both NAPE and IsoLG-PE have large aliphatic headgroups, we hypothesized that NAPE-PLD might also hydrolyze IsoLG-PE.

We tested this hypothesis by transfecting HEK293 cells with siRNA specific for NAPE-PLD before treating the cells with 1 μM IsoLG to form IsoLG-PE and then once again measuring the rate of IsoLG-PE hydrolysis at 1 h posttreatment. Transfection with siRNA targeting human NAPE-PLD markedly reduced both NAPE-PLD mRNA and protein levels compared with cells transfected with negative control siRNA (Fig. 3A, B). In cells transfected with control siRNA, IsoLG-PE levels were significantly reduced 1 h posttreatment compared with immediately after treatment. In contrast, in cells transfected with NAPE-PLD siRNA, IsoLG-PE levels at 1 h posttreatment were similar to those found immediately following treatment (Fig. 3C), suggesting that the loss of IsoLG-PE seen in wild-type cells principally resulted from hydrolysis by NAPE-PLD.

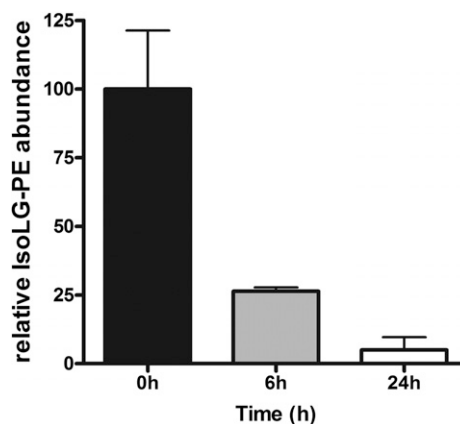


Fig. 2. HUVECs degrade IsoLG-PE. Cells were incubated with IsoLG (1 μM) for 1 h at 37°C to form IsoLG-PE, excess IsoLG was removed by washing, and IsoLG-PE levels were measured at 0, 6, or 24 h postwash by LC-MS. Bars represent mean \pm SEM, $n = 2$, one-way ANOVA, $P = 0.0259$.

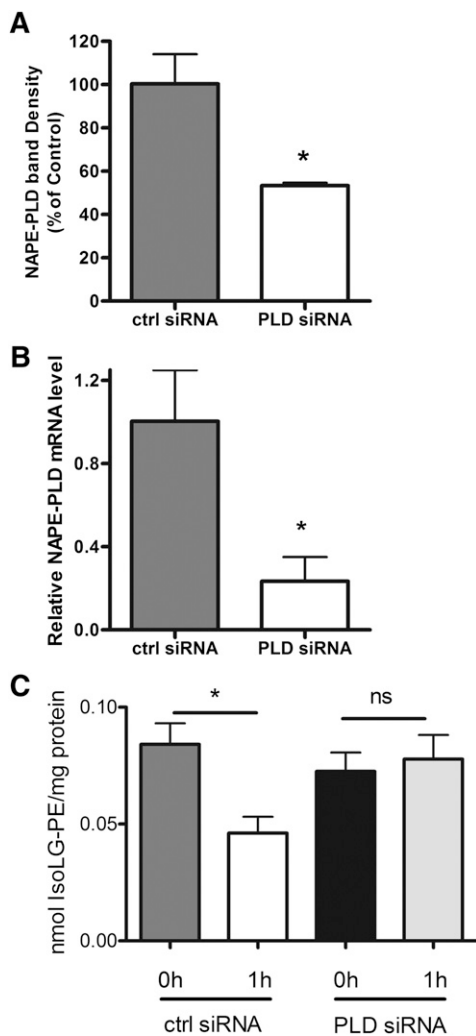


Fig. 3. Knockdown of NAPE-PLD in HEK293 cells inhibits degradation of IsoLG-PE. HEK293 cells were transfected either with control siRNA (ctrl siRNA) or with siRNA specific for NAPE-PLD (PLD siRNA) and the effect of NAPE-PLD knockdown on IsoLG-PE levels after incubation with IsoLG (1 μ M) was determined. **A:** Normalized immunoblot band density for NAPE-PLD relative to actin. Bars represent mean \pm SEM, $n = 3$, $*P = 0.272$ two-tailed t -test. **B:** Fold expression of NAPE-PLD mRNA relative to control siRNA-treated cells, measured by quantitative RT-PCR. Bars represent mean \pm SEM, $n = 3$, $*P = 0.477$ two-tailed t -test. **C:** Effect of NAPE-PLD knockdown on IsoLG-PE levels. Bars represent mean \pm SEM, $n = 3$; $*P = 0.0292$, 0 h versus 1 h postwash for control (ctrl) siRNA, two-tailed t -test; $P = 0.7109$ (ns), 0 h versus 1 h postwash for PLD siRNA, two-tailed t -test.

NAPE-PLD hydrolyzes IsoLG-PE to IsoLG-Etn

To confirm that NAPE-PLD hydrolyzes IsoLG-PE to IsoLG-Etn, we expressed and purified recombinant mouse NAPE-PLD (Fig. 4). We incubated this recombinant NAPE-PLD with synthetic IsoLG-PE for 1 h and assayed for the formation of IsoLG-Etn using our previously established MS assay (7–9). After 1 h incubation of IsoLG-PE with NAPE-PLD, we detected a large peak in the m/z 478 \rightarrow 152 ion chromatograph corresponding to IsoLG-Etn (Fig. 5A). Incubation of IsoLG-PE under these same conditions without enzyme did not generate a corresponding peak in the m/z 478 \rightarrow 152 ion chromatograph (Fig. 5B). The

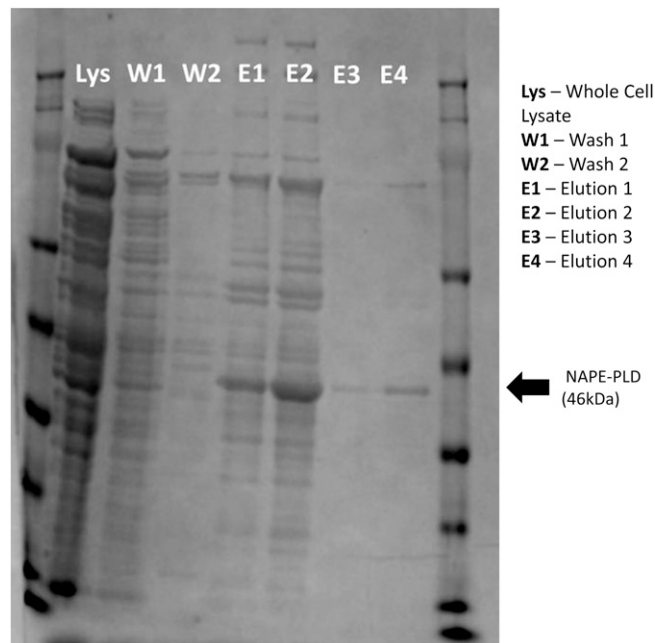


Fig. 4. Expression and purification of recombinant mouse NAPE-PLD from *E. coli*. DNA encoding mouse NAPE-PLD was inserted into the pQE-80 His vector and the resulting plasmid transformed into *E. coli*. Lysates (Lys) were then incubated with Ni-NTA agarose beads, washed two times (W1 and W2), and then eluted four times with 1 ml of elution buffer (E1, E2, E3, and E4, respectively.) An aliquot of each was run on SDS-PAGE and visualized with Coomassie blue stain. The major protein in the E3 and E4 fractions was a protein at 46 kDa, matching the expected size for NAPE-PLD.

retention time of the NAPE-PLD hydrolysis product was identical to that of synthetic [$^2\text{H}_4$]IsoLG-Etn (Fig. 5C). These findings confirmed that NAPE-PLD hydrolyzes IsoLG-PE to IsoLG-Etn.

IsoLG-PE is a competitive inhibitor of NAPE hydrolysis by NAPE-PLD

Because NAPE-PLD generates analogous products for both NAPE and IsoLG-PE, we considered the possibility that these two compounds might compete for binding to the same site in NAPE-PLD. To test this hypothesis, we used a fluorophore-labeled NAPE analog, NBD-NAPE, and monitored the hydrolysis reaction by formation of NBD-PA. When NBD-NAPE (10 μ M) was incubated with recombinant NAPE-PLD in the presence of IsoLG-PE (0–100 μ M), we found that IsoLG-PE dose-dependently reduced NBD-NAPE hydrolysis (Fig. 6A). A 10:1 ratio of IsoLG-PE to NBD-NAPE completely inhibited NBD-NAPE hydrolysis. To confirm that this competitive inhibition was not due to poor utilization of the fluorescently labeled NBD-NAPE, we examined the kinetics of NAPE-PLD-mediated NBD-NAPE hydrolysis. We found that the K_m for NAPE-PLD of the fluorescent analog of NAPE to be 3.79 μ M, with the V_{max} as 49 $\text{nmol min}^{-1} \text{mg}^{-1}$ NAPE-PLD (Fig. 6B). Thus the calculated catalytic efficiency (V_{max}/K_m) for NBD-NAPE hydrolysis under these conditions (12.9 $\text{ml min}^{-1} \text{mg}^{-1}$) is comparable to that reported for native NAPE hydrolysis (29.7 $\text{ml min}^{-1} \text{mg}^{-1}$) (16), suggesting that NBD-labeling only marginally alters efficiency of NAPE-PLD

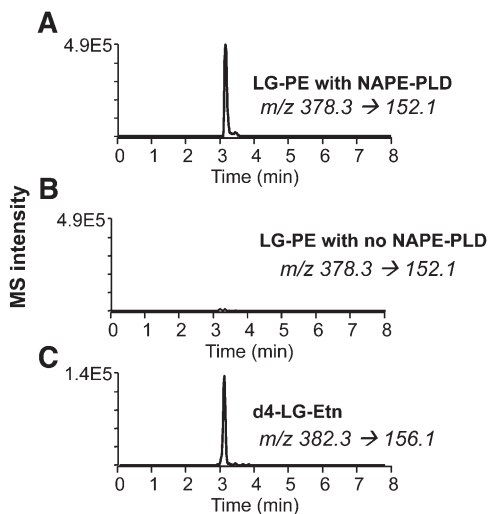


Fig. 5. NAPE-PLD hydrolyzes IsoLG-PE to IsoLG-Etn. IsoLG-PE was incubated with NAPE-PLD (A) or without NAPE-PLD (B) and the extent of IsoLG-Etn formation determined by MS using MRM at m/z 378.3 \rightarrow 152.1. C: MRM analysis at m/z 382.3 \rightarrow 156.1 for synthetic d4-IsoLG-Etn in this same chromatographic system.

hydrolysis. We then determined the catalytic efficiency of NBD-IsoLG-PE hydrolysis using the same HPLC-coupled fluorometric assay for NBD-PA. We found that NBD-IsoLG-PE has a K_m of 1.56 μM and a V_{max} of 5.96 $\text{nmol min}^{-1} \text{mg}^{-1}$, yielding a catalytic efficiency of 3.85 $\text{ml min}^{-1} \text{mg}^{-1}$ (Fig. 6C). These results support the notion that IsoLG-PE, like NAPE, is a substrate for NAPE-PLD and competes for the same substrate binding site.

IsoLG-Etn is an intermediate product of IsoLG-PE hydrolysis

We next examined the stability of IsoLG-Etn generated from IsoLG-PE. In HEK293 cells, we found that IsoLG-Etn levels did not accumulate despite the decrease of IsoLG-PE over the 6 h period (Fig. 7A). To test if HEK293 cells had IsoLG-Etn degrading activity, we prepared lysates from untreated HEK293 cells and then added synthetic IsoLG-Etn to these lysates and monitored IsoLG-Etn levels over time. We found that IsoLG-Etn decreased by 56% with 1 h incubation (Fig. 7B), clearly indicating that HEK293 cells possess enzymatic activity to degrade IsoLG-Etn. We did not find further degradation with longer incubations, which may reflect the instability of the IsoLG-Etn degrading enzyme(s) in the lysate.

DISCUSSION

While the formation of a family of al-PEs including IsoLG-PE has been recently established (11, 18), the mechanism by which these compounds are metabolized has been unknown. Our studies demonstrate that cells utilize NAPE-PLD to rapidly degrade IsoLG-PE to IsoLG-Etn, which then undergoes further metabolism (Fig. 8). IsoLG-PE is 10 times more potent than IsoLG-Etn at promoting activation of endothelial cells (9), so this initial step in the

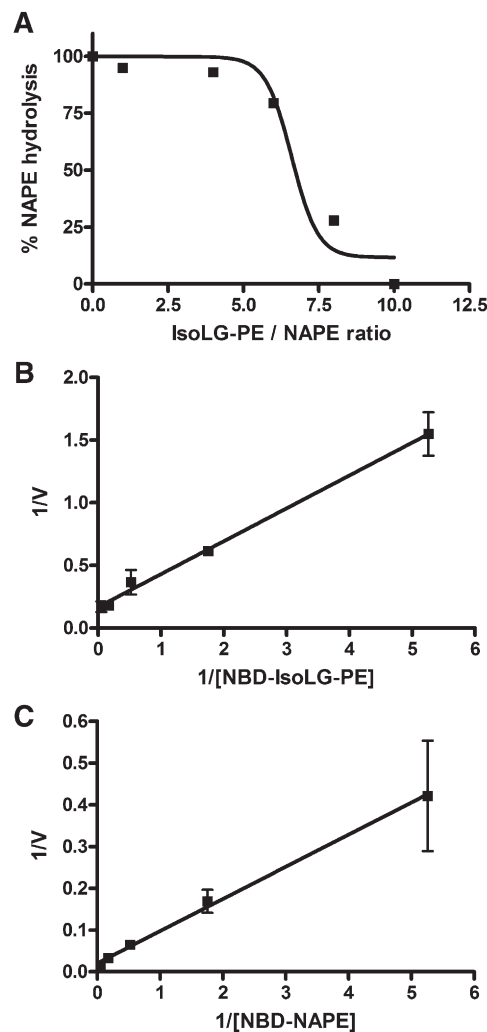


Fig. 6. Kinetic studies of NAPE-PLD hydrolysis of IsoLG-PE and NAPE. Fluorescently labeled NBD-NAPE and NBD-IsoLG-PE were used to measure the rate of hydrolysis of each substrate to NBD-phosphatidate (NBD-PA), analyzed by fluorescence-coupled HPLC (460 nm excitation/530 nm emission). A: IsoLG-PE inhibits hydrolysis of NBD-NAPE by recombinant NAPE-PLD. IsoLG-PE (0–100 μM) was incubated with NAPE-PLD and 10 mM NBD-NAPE and the resulting rate of hydrolysis normalized to the rate without IsoLG-PE. B: Lineweaver-Burke plot of the concentration dependence for the rate of hydrolysis of NBD-NAPE by NAPE-PLD. Calculated K_m = 3.79 μM , calculated V_{max} = 49 $\text{nmol min}^{-1} \text{mg}^{-1}$. C: Lineweaver-Burke plot of the concentration dependence for the rate of hydrolysis of NBD-IsoLG-PE by NAPE-PLD.

degradation of IsoLG-PE should provide substantial protection to the cells, while subsequent degradation of IsoLG-Etn would further enhance this protection. These studies suggest that NAPE-PLD activity promotes an anti-inflammatory state in two ways: first, by conversion of NAPE to anti-inflammatory NAEs such as oleoylethanolamide and palmitoylethanolamide, and second, by degrading pro-inflammatory lipids such as IsoLG-PE to their nonactive metabolites.

Previous characterization of the substrates for NAPE-PLD found that NAEs with saturated *N*-acyl chains of C4 to C20 are hydrolyzed efficiently, that NAEs with *N*-acyl chains of polyunsaturated fatty acids are hydrolyzed only

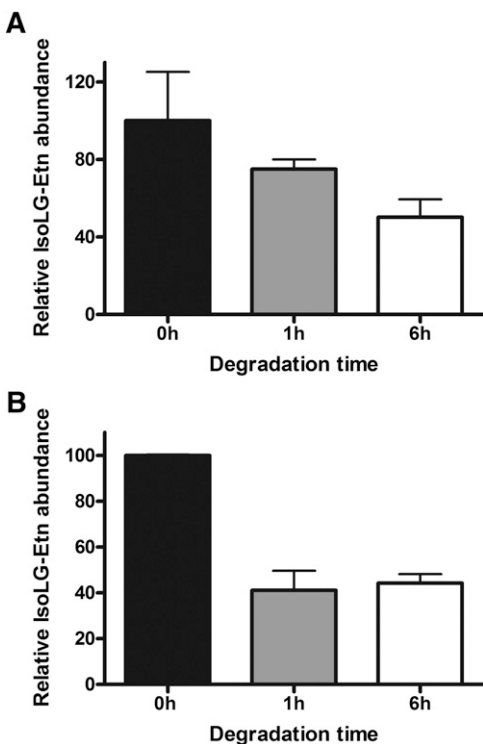


Fig. 7. Metabolism of IsoLG-Etn by HEK293 cells. A: Relative levels of IsoLG-Etn over time in IsoLG pretreated HEK293 cells. Confluent HEK293 cells were incubated with IsoLG (1 μ M) for 1 h to form IsoLG-PE, excess IsoLG was removed by washing with DMEM, and IsoLG-Etn levels were measured at 0, 1, or 6 h postwash by LC-MS. Bars represent mean \pm SEM, $n = 3$, one-way ANOVA, $P = 0.1618$. B: Relative levels of IsoLG-Etn over time after incubation with HEK293 cell lysate. Lysates were prepared from HEK293 cells and synthetic IsoLG-Etn added for 0 to 6 h. After extraction, the levels of IsoLG-Etn remaining were determined by LC-MS. Bars represent mean \pm SEM, $n = 2$, one-way ANOVA, $P = 0.0077$.

slightly less efficiently, but that PC, PE, phosphatidylserine, and phosphatidylinositol are not hydrolyzed to any appreciable extent (16). NAPE-PLD hydrolyzed *N*-acyl-lyso-PE with a catalytic efficiency that was 31% of NAPE (16) and we found that it hydrolyzed IsoLG-PE with a similar efficiency (30% that of NAPE). These findings suggest that the substrate binding pocket of NAPE-PLD is sufficiently promiscuous to accommodate a range of PEs modified with aliphatic headgroups and that more polar modified PEs are simply hydrolyzed at a somewhat slower rate.

Our studies raise the possibility that NAPE-PLD functions as a PLD for hydrolysis of *N*-modified PE formed by a number of biochemical pathways, including lipid peroxidation. NAPE-PLD was originally characterized as a key enzyme in the formation of the endocannabinoid anandamide via NAPE hydrolysis. However, while genetic deletion of NAPE-PLD decreased the levels of oleoylethanolamide and palmitoylethanolamide, it did not decrease anandamide levels in mice, suggesting that anandamide synthesis is not the major function of NAPE-PLD (17). If instead, NAPE-PLD's major role is to guard against inflammation and oxidant injury by acting as a promiscuous PLD for *N*-modified PE, NAPE-PLD would be expected to

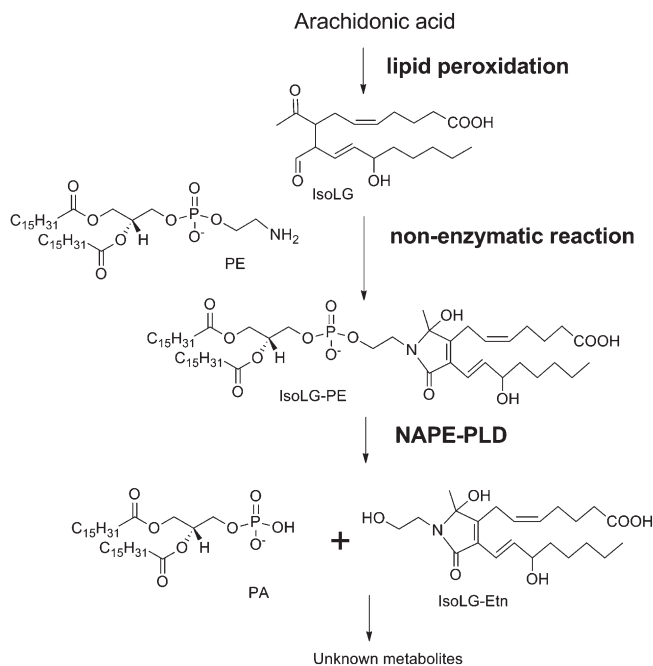


Fig. 8. Schematic of IsoLG-PE metabolism. Lipid peroxidation of arachidonic acid generates a variety of lipid aldehydes including IsoLG. IsoLG reacts rapidly with PE to form IsoLG-PE, which is proinflammatory and cytotoxic. NAPE-PLD hydrolyzes IsoLG-PE to the less toxic metabolite IsoLG-Etn and then IsoLG-Etn is further metabolized by unknown mechanisms.

be highly expressed in tissue sensitive to oxidative injury and to be induced acutely by oxidative injury. Consistent with this expectation, NAPE-PLD is widely expressed, with the highest expression in tissues such as brain, kidney, and testis that are particularly sensitive to oxidative injury (16). In brain, NAPE-PLD localizes to a variety of brain cells including neurons, astrocytes, cerebral endothelial cells, and microglia (19). Interestingly, at least in hippocampal mossy fibers, NAPE-PLD is preferentially localized to the cisternae of smooth endoplasmic reticulum (20). This subcellular localization may be of particular importance given our previous observation that IsoLG-PE is quickly trafficked to the endoplasmic reticulum (9). Also consistent with a potential role in preventing oxidative damage, NAPE-PLD expression is acutely upregulated in response to spinal cord contusion in rats (21).

Together these observations suggest the need for future studies to examine the contribution of NAPE-PLD to modulating oxidative injury. For instance, are other al-PEs besides IsoLG-PE also degraded by NAPE-PLD and does the loss of NAPE-PLD activity make cells and organisms vulnerable to diseases associated with oxidative injury? Such studies will be particularly helpful in understanding the contribution of PE modification to the overall effects of lipid aldehydes, because modulating al-PE levels via NAPE-PLD activity would not affect the extent of protein and DNA modification by these same lipid aldehydes. Thus our discovery that NAPE-PLD metabolizes IsoLG-PE is an important step toward understanding the biological importance of IsoLG-PE and other al-PEs. **■**

REFERENCES

- Salomon, R. G., D. B. Miller, M. G. Zagorski, and D. J. Coughlin. 1984. Solvent-induced fragmentation of prostaglandin endoperoxides. New aldehyde products from PGH₂ and a novel intramolecular 1,2-hydride shift during endoperoxide fragmentation in aqueous solution. *J. Am. Chem. Soc.* **106**: 6049–6060.
- Salomon, R. G., and D. B. Miller. 1985. Levuglandins: isolation, characterization, and total synthesis of new secoprostanoid products from prostaglandin endoperoxides. *Adv. Prostaglandin Thromboxane Leukot. Res.* **15**: 323–326.
- Fukuda, K., S. S. Davies, T. Nakajima, B. H. Ong, S. Kupersmidt, J. Fessel, V. Amarnath, M. E. Anderson, P. A. Boyden, P. C. Viswanathan, et al. 2005. Oxidative mediated lipid peroxidation recapitulates proarrhythmic effects on cardiac sodium channels. *Circ. Res.* **97**: 1262–1269.
- Hoppe, G., G. Subbanagounder, J. O'Neil, R. G. Salomon, and H. F. Hoff. 1997. Macrophage recognition of LDL modified by levuglandin E2, an oxidation product of arachidonic acid. *Biochim. Biophys. Acta.* **1344**: 1–5.
- Bernoud-Hubac, N., D. A. Alam, J. Lefils, S. S. Davies, V. Amarnath, M. Guichardant, L. J. Roberts 2nd, and M. Lagarde. 2009. Low concentrations of reactive gamma-ketoaldehydes prime thromboxane-dependent human platelet aggregation via p38-MAPK activation. *Biochim. Biophys. Acta.* **1791**: 307–313.
- Davies, S. S., V. Amarnath, K. S. Montine, N. Bernoud-Hubac, O. Boutaud, T. J. Montine, and L. J. Roberts 2nd. 2002. Effects of reactive gamma-ketoaldehydes formed by the isoprostane pathway (isoketals) and cyclooxygenase pathway (levuglandins) on proteasome function. *FASEB J.* **16**: 715–717.
- Bernoud-Hubac, N., L. B. Fay, V. Amarnath, M. Guichardant, S. Bacot, S. S. Davies, L. J. Roberts II, and M. Lagarde. 2004. Covalent binding of isoketals to ethanolamine phospholipids. *Free Radic. Biol. Med.* **37**: 1604–1611.
- Sullivan, C. B., E. Matafonova, L. J. Roberts II, V. Amarnath, and S. S. Davies. 2010. Isoketals form cytotoxic phosphatidylethanolamine adducts in cells. *J. Lipid Res.* **51**: 999–1009.
- Guo, L., Z. Chen, B. E. Cox, V. Amarnath, R. F. Epand, R. M. Epand, and S. S. Davies. 2011. Phosphatidylethanolamines modified by γ -ketoaldehyde (γ KA) induce endoplasmic reticulum stress and endothelial activation. *J. Biol. Chem.* **286**: 18170–18180.
- Hidalgo, F. J., F. Nogales, and R. Zamora. 2004. Determination of pyrrolized phospholipids in oxidized phospholipid vesicles and lipoproteins. *Anal. Biochem.* **334**: 155–163.
- Li, W., J. M. Laird, L. Lu, S. Roychowdhury, L. E. Nagy, R. Zhou, J. W. Crabb, and R. G. Salomon. 2009. Isolevuglandins covalently modify phosphatidylethanolamines in vivo: Detection and quantitative analysis of hydroxylactam adducts. *Free Radic. Biol. Med.* **47**: 1539–1552.
- Guo, L., V. Amarnath, and S. S. Davies. 2010. A liquid chromatography-tandem mass spectrometry method for measurement of N-modified phosphatidylethanolamines. *Anal. Biochem.* **405**: 236–245.
- Okamoto, Y., J. Morishita, J. Wang, P. C. Schmid, R. J. Krebsbach, H. H. Schmid, and N. Ueda. 2005. Mammalian cells stably overexpressing N-acylphosphatidylethanolamine-hydrolysing phospholipase D exhibit significantly decreased levels of N-acylphosphatidylethanolamines. *Biochem. J.* **389**: 241–247.
- Petersen, G., and H. S. Hansen. 1999. N-acylphosphatidylethanolamine-hydrolysing phospholipase D lacks the ability to transphosphatidylate. *FEBS Lett.* **455**: 41–44.
- Wang, J., Y. Okamoto, J. Morishita, K. Tsuboi, A. Miyatake, and N. Ueda. 2006. Functional analysis of the purified anandamide-generating phospholipase D as a member of the metallo-beta-lactamase family. *J. Biol. Chem.* **281**: 12325–12335.
- Okamoto, Y., J. Morishita, K. Tsuboi, T. Tonai, and N. Ueda. 2004. Molecular characterization of a phospholipase D generating anandamide and its congeners. *J. Biol. Chem.* **279**: 5298–5305.
- Leung, D., A. Saghatelian, G. M. Simon, and B. F. Cravatt. 2006. Inactivation of N-acyl phosphatidylethanolamine phospholipase D reveals multiple mechanisms for the biosynthesis of endocannabinoids. *Biochemistry.* **45**: 4720–4726.
- Guo, L., Z. Chen, V. Amarnath, and S. S. Davies. 2012. Identification of novel bioactive aldehyde-modified phosphatidylethanolamines formed by lipid peroxidation. *Free Radic. Biol. Med.* **53**: 1226–1238.
- Zhang, H., D. A. Hilton, C. O. Hanemann, and J. Zajicek. 2011. Cannabinoid receptor and N-acyl phosphatidylethanolamine phospholipase D—evidence for altered expression in multiple sclerosis. *Brain Pathol.* **21**: 544–557.
- Nyilas, R., B. Dudok, G. M. Urban, K. Mackie, M. Watanabe, B. F. Cravatt, T. F. Freund, and I. Katona. 2008. Enzymatic machinery for endocannabinoid biosynthesis associated with calcium stores in glutamatergic axon terminals. *J. Neurosci.* **28**: 1058–1063.
- Garcia-Ovejero, D., A. Arevalo-Martin, S. Petrosino, F. Docagne, C. Hagen, T. Bisogno, M. Watanabe, C. Guaza, V. Di Marzo, and E. Molina-Holgado. 2009. The endocannabinoid system is modulated in response to spinal cord injury in rats. *Neurobiol. Dis.* **33**: 57–71.